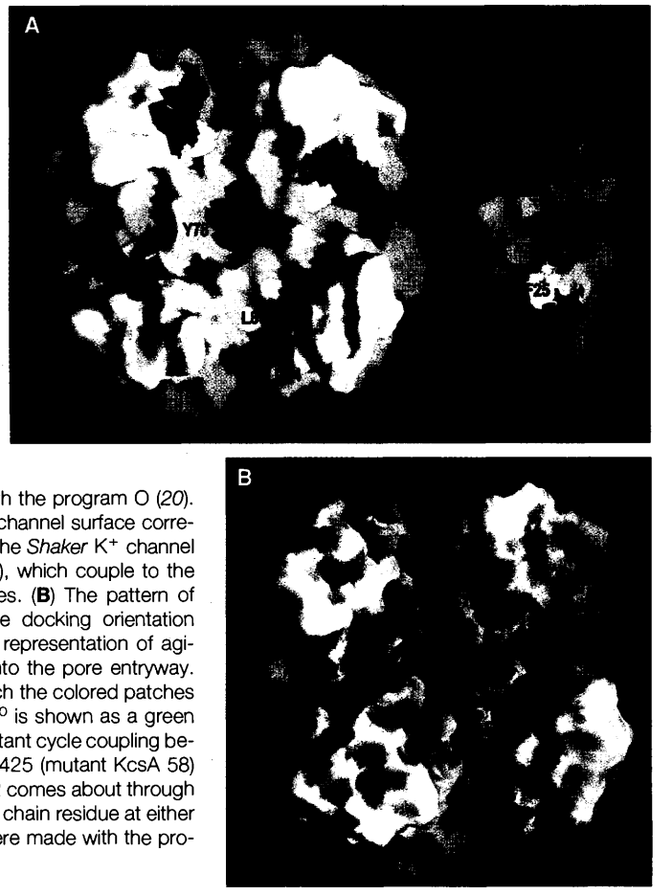

Fig. 4. Docking of agitoxin2 onto the KcsA K^+ channel. (**A**) Molecular surface of the pore entryway of the KcsA K^+ channel (left) and agitoxin2 (right). The colors indicate locations of interacting residues on the toxin and channel surfaces as determined by thermodynamic mutant cycle analysis of the *Shaker* K^+ channel-agitoxin2 interaction (*4*, *8*). The three pore mutations of the KcsA K^+ channel used in this study (Q58A, T61S, and R64D) were introduced into the channel model with the program O (*20*). Indicated residues on the channel surface correspond to the positions of the *Shaker* K^+ channel equivalent residues (Fig. 1), which couple to the indicated agitoxin2 residues. (**B**) The pattern of colors in (A) suggests the docking orientation shown by the main chain representation of agitoxin2 placed manually onto the pore entryway. The side chain colors match the colored patches in (A). The position of Gly^{10} is shown as a green band on agitoxin2. The mutant cycle coupling between residues at *Shaker* 425 (mutant KcsA 58) and residue 10 of agitoxin2 comes about through substitution of a bulky side chain residue at either position (*4*, *7*). Pictures were made with the program GRASP (*19*).

18. A. M. Krezel *et al.*, *Prot. Sci.* **4** 1478 (1995).
19. A. Nicholls, K. A. Sharp, B. Honig, *Proteins* **11**, 281 (1991).
20. T. A. Jones, J. Y. Zou, J. Y. Cowan, M. Kjeldgaard, *Acta Crystallogr.* **A47**, 110 (1991).
21. We thank J. Gulbis, J. P. Imredy, and D. A. Doyle for assistance in preparation of the figures and helpful discussions on the work. Supported by NIH GM43949. R.M. is an investigator in the Howard Hughes Medical Institute.

6 March 1998; accepted 13 March 1998

Requirement of Ras-GTP–Raf Complexes for Activation of Raf-1 by Protein Kinase C

Richard Marais, Yvonne Light, Clive Mason, Hugh Paterson, Michael F. Olson, Christopher J. Marshall*

Receptor tyrosine kinase–mediated activation of the Raf-1 protein kinase is coupled to the small guanosine triphosphate (GTP)–binding protein Ras. By contrast, protein kinase C (PKC)–mediated activation of Raf-1 is thought to be Ras independent. Nevertheless, stimulation of PKC in COS cells led to activation of Ras and formation of Ras–Raf-1 complexes containing active Raf-1. Raf-1 mutations that prevent its association with Ras blocked activation of Raf-1 by PKC. However, the activation of Raf-1 by PKC was not blocked by dominant negative Ras, indicating that PKC activates Ras by a mechanism distinct from that initiated by activation of receptor tyrosine kinases.

The PKC family of lipid-dependent Ser-Thr kinases has at least 11 members (*1*). The typical and atypical PKC isozymes are activated by diacylglycerol (DAG), which is produced by the metabolism of phosphatidyl inositols. In the case of 7-transmembrane (7-TM) receptors that are coupled to the heterotrimeric guanosine nucleotide–binding protein (G protein) Gαq, DAG is generated by the activation of phospholipase C-β (PLC-β) (*2*). Both the typical and atypical PKCs are activated by phorbol esters. Activation of PKC leads to short-term responses such as altered metabolic activity and to long-term responses such as differentiation or effects on proliferation and apoptosis (*1*). The extracellular signal–regulated kinases (ERKs) are mitogen-activated protein kinases (MAPKs), which are activated by PKC (*3*–*7*) and appear to mediate the effects of PKC on differentiation, secretion, proliferation, and hypertrophy (*8*). Signaling from receptor tyrosine kinases to ERKs is dependent on Ras proteins and the protein kinase Raf-1 (*9*). However, the role of Ras in transducing signals from PKC to the ERKs is unclear, because expression of a dominant negative Ras in which amino acid 17 is changed to Asn (N17Ras) does not block ERK activation by PKC in a number of cell types (*4*, *5*). This Ras mutant, which is thought to function by inhibiting guanine nucleotide exchange factors (*10*), blocks activation of ERKs in response to stimulation of receptor tyrosine kinases in many cell types (*4*–*6*).

To investigate whether PKC activates the ERK MAPK pathway by a mechanism independent of Ras, we used a monkey kidney cell line (COS cells), because in these cells, N17Ras does not block PKC-mediated ERK activation (*4*). We blocked Ras signaling by microinjection of the Ras-neutralizing monoclonal antibody Y13-259 (*11*). To detect ERK activation, we used an antibody that recognizes only the dually phosphorylated, active form of ERK. Activation of ERK in COS cells treated with 12-O-tetradecanoyl-phorbol-13-acetate (TPA) was completely blocked by microinjection of Y13-259 (Fig. 1). This demonstrates an essential role for Ras in activation of the ERK MAPK cascade by PKC. These data are consistent with studies on overexpression of Ras guanosine triphosphatase–activating protein (p120Ras-GAP), which blocks TPA-stimulated activation of ERKs, although it is unclear in those studies whether the p120Ras-GAP was acting on Ras or a related protein (*7*).

To further investigate whether Ras has a role in activation of Raf-1 by PKC, we used a mutant Raf-1 protein in which Arg^{89} is replaced with Leu (R89LRaf-1). This mutant does not bind the GTP-bound form of Ras (Ras-GTP) (*12*). Unlike transiently expressed wild-type Raf-1 (mRaf-1), R89LRaf-1 was not activated in cells treated with TPA (Fig. 2A). Exogenous mRaf-1 was activated with similar

CRC Centre for Cell and Molecular Biology, Institute of Cancer Research, 237 Fulham Road, London SW3 6JB, UK.

*To whom correspondence should be addressed. E-mail: chrism@icr.ac.uk

kinetics to those of the endogenous protein (*13*), and activation was blocked in cells treated with the PKC inhibitor Ro 31-8220 (Fig. 2B) (*14*). Ro 31-8220 had only a small effect on activation of mRaf-1 in cells treated with epidermal growth factor (EGF) (Fig. 2B). Expression of N17Ras, which has no effect on ERK activation in COS cells treated with TPA (*4*), did not block activation of mRaf-1 following TPA treatment, but did block mRaf-1 activation in response to EGF (Fig. 2B). To show that activation of Raf-1 by a physiological activator of PKC also depends on Ras, we examined the activation of mRaf-1 in cells expressing human muscarinic type 1 receptor (Hm1), which is coupled to Gαq (*15*). There was no activation of R89LRaf-1 when the Hm1 receptor was activated in cells treated with carbachol (Fig. 2A), whereas wild-type mRaf-1 was activated 8- to 10-fold in an Ro 31-8220–sensitive but N17Ras-insensitive manner (Fig. 2B). The inability of R89LRaf-1 to be activated by tyrosine kinase signaling can be overcome by targeting it to the plasma membrane with a CAAX motif (*16, 17*). R89LRafCAAX was activated in cells treated with TPA (Fig. 2C), which shows that activation of Raf-1 by PKC requires Ras-GTP–mediated translocation to the plasma membrane, but that additional events at the membrane are required for full activation.

The requirement of Ras in the activation of Raf-1 is consistent with observation that mutations in the Ras-binding domain (RBD) and Cys-rich domain of Raf-1 affect its activation by EGF and TPA (*18*). However, our results differ from those showing that R89LRaf-1 is activated by EGF and TPA (*19*). To further examine the role of Ras in Raf-1 activation by PKC, we investigated whether Ras–Raf-1 complexes form in cells treated with TPA. Endogenous Ras was immunoprecipitated from extracts of TPA-treated cells, using the rat monoclonal antibody Y13-238, which can immunoprecipitate Ras-GTP–Raf complexes from Ras-transformed or EGF-stimulated cells (*20*). The immunoprecipitates were analyzed for association of endogenous Raf-1 by immunoblotting. We also performed a reciprocal analysis by immunoprecipitating endogenous Raf-1. In cells treated with TPA, complexes were formed between Ras and Raf-1 (Fig. 3A).

To determine whether the Raf-1 associated with Ras from TPA-stimulated cells was active, we tested whether the Y13-238 immunoprecipitates could activate a glutathione-S transferase (GST)–tagged version of the kinase activator of ERK, Mek-1 (GST-Mek-1). Ras immunoprecipitates from TPA-stimulated cells activated GSTMek-1 (Fig. 3B). Approximately 65% of this activity could be eluted by treating the immunoprecipitates with buffers containing high concentrations of salt; of this, 50% could be reprecipitated with a monoclonal antibody to Raf-1 (Fig. 3B). Thus, Raf-1 from TPA-stimulated cells forms a complex with Ras and is activated.

Formation of complexes between Ras and Raf-1 requires that Ras be in the GTP-bound form (*20, 21*). Therefore, we examined whether activation of PKC leads

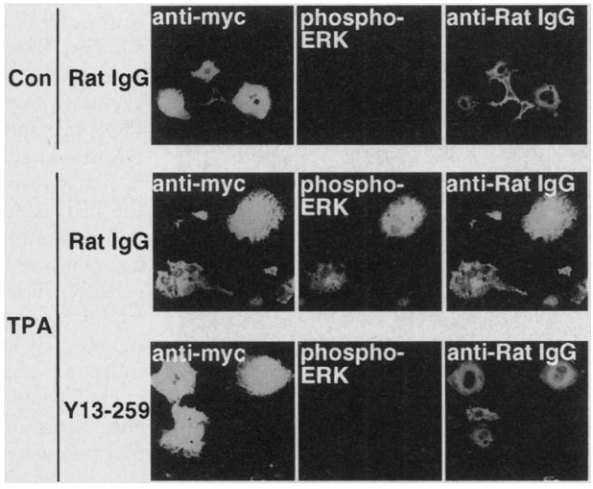

Fig. 1. Requirement of Ras for activation of ERK by PKC. COS cells were microinjected with an expression vector for myc-tagged ERK2 together with either control rat immunoblobulin G (IgG) (top and middle panels) or with Y13-259 (bottom panels). The cells were deprived of serum (Con) or stimulated with TPA for 20 min as indicated. Staining with the 9E10 monoclonal antibody to myc (anti-Myc) and with an antibody to rat IgG (anti-Rat IgG) were used to reveal the injected cells. Activated ERK was detected with an antibody that recognizes dually-phosphorylated ERK (phospho-ERK; Promega, no. V6671). For each treatment, identical fields of cells are shown stained with the three antisera.

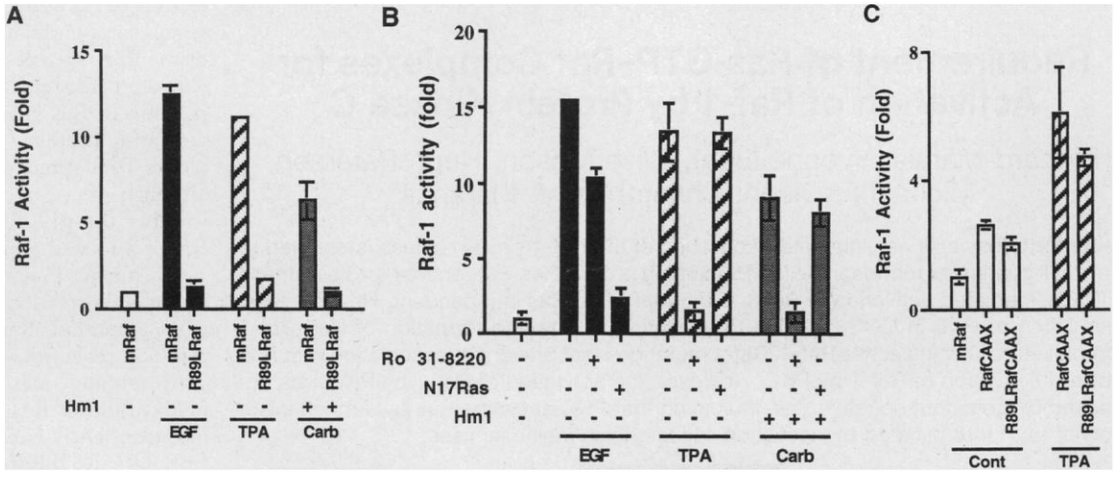

Fig. 2. Activation of mRaf-1 by PKC. (**A**) Activation of Raf-1 by PKC requires Raf-1 interaction with Ras. mRaf-1 or R89LRaf-1 were expressed in COS cells (*17*) alone or together with Hm1 as indicated. The cells were deprived of serum for 24 hours and stimulated for 20 min with EGF (10 ng/ml), TPA (40 nM), or carbachol (Carb, 100 μM). The activity of mRaf-1 was measured from COS cell extracts by immunoprecipitation with the 9E10 monoclonal antibody and kinase cascade assay, using GSTMek-1, GSTERK2, and myelin basic protein as substrates (*24*). In the absence of added GSTMek-1, GSTERK2 was not activated (*13*). The results shown are for a representative experiment assayed in triplicate and are corrected for background counts (immunoprecipitations done with control antibodies). Error bars show standard deviations. One unit of activity represents mRaf-1 activity from cells deprived of serum. Similar results were obtained in three independent experiments. (**B**) Requirement of PKC for activation of Raf-1 by TPA and Hm1. mRaf-1 was expressed in COS cells alone or together with N17Ras and Hm1 as indicated. Where indicated, the cells were pretreated with the PKC inhibitor Ro 31-8220 (10 μM for 10 min). Similar results were obtained in four independent experiments. (**C**) Activation of membrane-targeted Raf-1 by TPA. R89LRaf and R89LRafCAAX (*17*) were expressed in COS cells that were deprived of serum (Cont) or treated with TPA (TPA). Similar results were obtained in two independent experiments.

to increased amounts of Ras-GTP by monitoring association between Ras-GTP and the Ras-binding domain of Raf-1 (*22*, *23*). Small amounts of Ras-GTP were detected in cells deprived of serum (Fig. 4A). Treatment of cells with TPA or EGF activated Ras to similar extents, but the response was slower with TPA, continuing to rise for 40 min after stimulation (Fig. 4A). The activation of Ras in response to TPA was blocked by the PKC inhibitor Ro 31-8220, whereas the activation in response to EGF was not (Fig. 4B). Stimulation of the Hm1 receptor also activated Ras in a PKC-dependent manner (Fig. 4B). H-Ras, N-Ras, and K-Ras were all activated in cells treated with TPA (*13*). The kinetics of the increases in Ras-GTP formation following TPA treatment were similar to those of increases in Raf-1 activity (Fig. 4C).

Our data show that Raf-1 activation by signals that activate PKC is a consequence of Ras activation and the formation of Ras-GTP–Raf-1 complexes. Although Raf-1 activation by PKC is mediated through Ras activation, it differs from activation by receptor tyrosine kinases in that it is not blocked by N17Ras. This observation emphasizes that the absence of an effect of N17Ras expression cannot be used to conclude that Ras is not part of a signaling pathway. Rather, our results indicate that Ras activation is a component of PKC signaling.

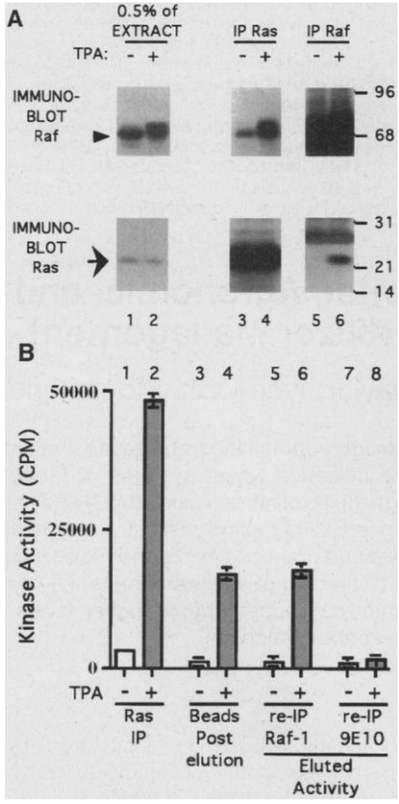

Fig. 3. Formation of Ras–Raf-1 complexes. Cells deprived of serum (–) or treated with TPA (+) for 60 min were extracted in medium-salt buffers, and endogenous Ras or Raf-1 was immunoprecipitated (*25*). (**A**) Immunoblot analysis of Ras-Raf complexes. Upper panels show immunoblots for Raf-1, and lower panels show immunoblots for Ras. Lanes 1 and 2: 0.5% of total cell extract; lanes 3 and 4: immunoprecipitation of Ras; lanes 5 and 6: immunoprecipitation of Raf-1. Molecular size markers (in kilodaltons) are shown to the right. (**B**) Association of Raf-1 activity with Ras. Y13-238 immunoprecipitates from cells deprived of serum (–) or treated with TPA (+) were analyzed for Mek activators in the kinase cascade assay (*17*). Lanes 1 and 2: Ras-associated GSTMek activator. Lanes 3 and 4: Ras immunocomplexes treated with high salt concentrations to elute the Mek activator (*25*); the amount of activator remaining associated with the immunoprecipitated Ras after elution was measured by returning the beads to a kinase assay. Lanes 5 through 8: reprecipitation of the Mek activator from parallel samples with a monoclonal antibody to Raf-1 (lanes 5 and 6) or with the 9E10 monoclonal antibody as a control (lanes 7 and 8). The assays were done in triplicate, and similar results were observed in two independent experiments. CPM, counts per minute.

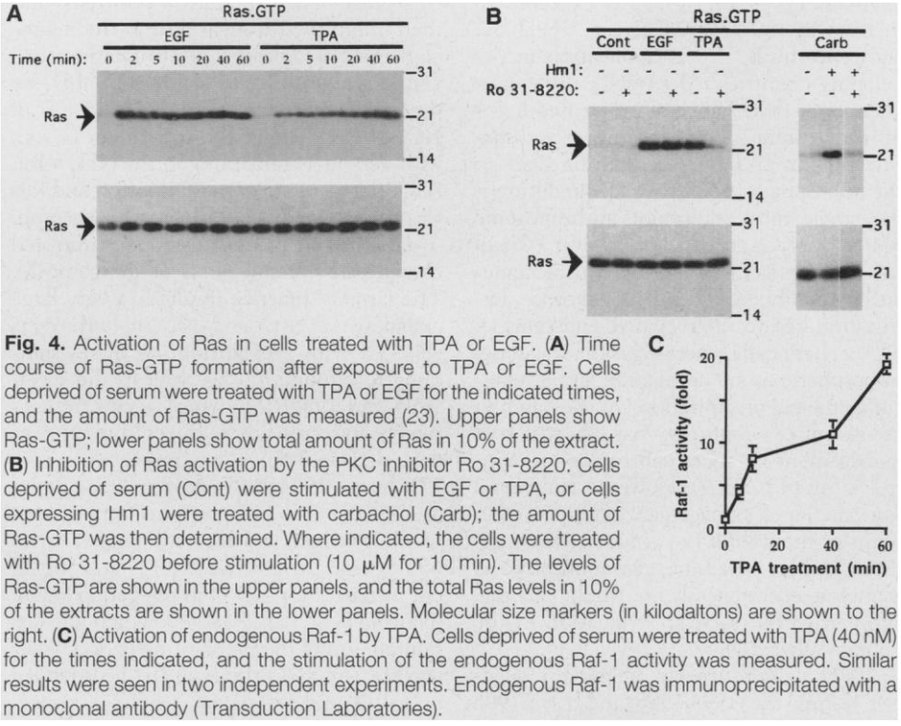

Fig. 4. Activation of Ras in cells treated with TPA or EGF. (**A**) Time course of Ras-GTP formation after exposure to TPA or EGF. Cells deprived of serum were treated with TPA or EGF for the indicated times, and the amount of Ras-GTP was measured (*23*). Upper panels show Ras-GTP; lower panels show total amount of Ras in 10% of the extract. (**B**) Inhibition of Ras activation by the PKC inhibitor Ro 31-8220. Cells deprived of serum (Cont) were stimulated with EGF or TPA, or cells expressing Hm1 were treated with carbachol (Carb); the amount of Ras-GTP was then determined. Where indicated, the cells were treated with Ro 31-8220 before stimulation (10 μM for 10 min). The levels of Ras-GTP are shown in the upper panels, and the total Ras levels in 10% of the extracts are shown in the lower panels. Molecular size markers (in kilodaltons) are shown to the right. (**C**) Activation of endogenous Raf-1 by TPA. Cells deprived of serum were treated with TPA (40 nM) for the times indicated, and the stimulation of the endogenous Raf-1 activity was measured. Similar results were seen in two independent experiments. Endogenous Raf-1 was immunoprecipitated with a monoclonal antibody (Transduction Laboratories).

REFERENCES AND NOTES

1. G. C. Blobe, S. Stribling, L. M. Obeid, Y. A. Hannun, in *Cell Signalling*, vol. 27 of *Cancer Surveys*, P. J. Parker and T. Pawson, Eds. (Cold Spring Harbor Laboratory Press, Cold Spring Harbor, NY, 1996), p. 213; L. V. Dekker and P. J. Parker, *Trends. Biochem. Sci.* **19**, 73 (1994); Y. Nishizuka, *Science* **258**, 607 (1992).
2. S. B. Lee and S. G. Rhee, *Curr. Opin. Cell. Biol.* **7**, 183 (1995); J. H. Exton, *Eur. J. Biochem.* **243**, 10 (1997).
3. S. J. Leevers, and C. J. Marshall, *EMBO J.* **11**, 569 (1992); S. Gupta, A. Weiss, G. Kumar, S. Wang, A. Nel, *J. Biol. Chem.* **269**, 17349 (1994).
4. L. R. Howe *et al.*, *Cell* **71**, 335 (1992); Y. Ueda *et al.*, *J. Biol. Chem.* **271**, 23512 (1996).
5. A. M. M. de Vries Smits, B. M. T. Burgering, S. J. Leevers, C. J. Marshall, J. L. Bos, *Nature* **357**, 602 (1992); B. E. Hawes, T. van Biesen, W. J. Koch, L. M. Luttrell, R. J. Lefkowitz, *J. Biol. Chem.* **270**, 17148 (1995); X. F. Ming *et al.*, *Nature* **371**, 426 (1994); T. van Biesen *et al.*, *J. Biol. Chem.* **271**, 1266 (1996).
6. K. W. Wood, C. Sarnecki, T. M. Roberts, J. Blenis, *Cell* **68**, 1041 (1992); S. M. Thomas, M. DeMarco, G. D'Arcangelo, S. Halegoua, J. S. Brugge, *ibid.*, p. 1031.
7. M. Nori, G. L'Allemain, M. J. Weber, *Mol. Cell. Biol.* **12**, 936 (1992).
8. Y. Zou *et al.*, *J. Biol. Chem.* **271**, 33592 (1996); A. Whelchel, J. Evans, J. Posada, *Am. J. Respir. Cell. Mol. Biol.* **16**, 589 (1997); F. K. Racke, K. Lewandowska, S. Goueli, A. N. Goldfarb, *J. Biol. Chem.* **272**, 23366 (1997); M. E. Cox and S. J. Parsons, *J. Neurochem.* **69**, 1119 (1997).
9. M. S. Marshall, *FASEB J.* **9**, 1311 (1995); D. K. Morrison and R. E. Cutler, *Curr. Opin. Cell. Biol.* **9**, 174 (1997); M. J. Robinson and M. H. Cobb, *ibid.*, p. 180.
10. L. A. Feig and G. M. Cooper, *Mol. Cell. Biol.* **8**, 3235 (1988); R. H. Medema, B. M. T. Burgering, J. L. Bos, *J. Biol. Chem.* **266**, 21186 (1991).
11. L. S. Mulcahy, M. R. Smith, D. W. Stacey, *Nature* **313**, 241 (1985).
12. J. R. Fabian, A. B. Vojtek, J. A. Cooper, D. K. Morrison, *Proc. Natl. Acad. Sci. U.S.A.* **91**, 5982 (1994).
13. R. Marais and C. J. Marshall, unpublished data.
14. P. D. Davis *et al.*, *J. Med. Chem.* **35**, 994 (1992).
15. D. E. Clapham and E. J. Neer, *Nature* **365**, 403 (1993).
16. D. Stokoe, S. G. Macdonald, K. Cadwallader, M. Symons, J. F. Hancock, *Science* **264**, 1463 (1994);

S. J. Leevers, H. F. Paterson, C. J. Marshall, *Nature* **369**, 411 (1994).
17. R. Marais, Y. Light, H. F. Paterson, C. J. Marshall, *EMBO J.* **14**, 3136 (1995).
18. Z. Lou, B. Diaz, M. S. Marshall, J. Avruch, *Mol. Cell. Biol.* **17**, 46 (1997).
19. H. Mischak *et al.*, *ibid.* **16**, 5409 (1996).
20. R. Finney and D. Herrera, *Methods Enzymol.* **255**, 310 (1995); B. Hallberg, S. I. Rayter, J. Downward, *J. Biol. Chem.* **269**, 3913 (1994).
21. L. Van Aelst, M. Barr, S. Marcus, A. Polverino, M. Wigler, *Proc. Natl. Acad. Sci. U.S.A.* **90**, 6213 (1993); S. A. Moodie, B. M. Willumsen, M. J. Weber, A. Wolfman, *Science* **260**, 1658 (1993); A. B. Vojtek, S. M. Hollenberg, J. A. Cooper, *Cell* **74**, 205 (1993); P. H. Warne, P. R. Viciana, J. Downward, *Nature* **364**, 352 (1993); H. Koide, T. Satoh, M. Nakafuku, Y. Kaziro, *Proc. Natl. Acad. Sci. U.S.A.* **90**, 8683 (1993).
22. S. J. Taylor and D. Shalloway, *Curr. Biol.* **6**, 1621 (1996).
23. J. de Rooij and J. Bos, *Oncogene* **14**, 623 (1997).
24. R. Marais, Y. Light, H. F. Paterson, C. S. Mason, C. J. Marshall, *J. Biol. Chem.* **272**, 4378 (1997).
25. All extraction procedures were done at 4°C. Cells were washed twice with phosphate-buffered saline, and each 10-cm dish of confluent cells was extracted in 300 μl of dilution buffer (*17*) containing 100 mM KCl and 5 mM $MgCl_2$, but only 0.05% v/v 2-mercaptoethanol (medium-salt buffer). DNA was sheared, and extracts were clarified by centrifugation (13,000*g* for 2 min); protein concentrations were measured with a Bio-Rad protein assay kit. Immunoblots for endogenous Ras or Raf-1 were done with monoclonal antibodies (products no. 02120 and no. R19120, Transduction Laboratories). For Ras-Raf complex analysis by immunoblot, endogenous Ras or Raf-1 was immunoprecipitated from ~15 mg of cellular protein with either 10 μg of Y13-238 or 10 μg of Raf-1 monoclonal antibody and probed by immunoblotting for Raf-1 or Ras. For assay of Ras-associated GSTMek-1 activation, Ras was immunoprecipitated from ~3.5 mg of cellular protein with Y13-238 (10 μg), washed four times with low-salt buffer, and assayed as described (*17*, *24*). Ras immunoprecipitates were eluted with extraction buffer (40 μl), diluted with dilution buffer (160 μl) (*17*), and reprecipitated with Raf-1 monoclonal antibody (2 μg). Measurements of Ras-GTP were done as described (*23*). The cells were extracted in medium-salt buffer, and proteins (~3 mg) were absorbed to bacterially expressed GSTRBD. Ras proteins were revealed by immunoblotting. In control experiments using GSTR89LRBD, Ras-GTP was not detected (*13*).

28 August 1997; accepted 17 February 1998

Integration of Environmental, Agronomic, and Economic Aspects of Fertilizer Management

Pamela A. Matson,* Rosamond Naylor, Ivan Ortiz-Monasterio

Nitrogen fertilization is a substantial source of nitrogen-containing trace gases that have both regional and global consequences. In the intensive wheat systems of Mexico, typical fertilization practices lead to extremely high fluxes of nitrous oxide (N_2O) and nitric oxide (NO). In experiments, lower rates of nitrogen fertilizer, applied later in the crop cycle, reduced the loss of nitrogen without affecting yield and grain quality. Economic analyses projected this alternative practice to save 12 to 17 percent of after-tax profits. A knowledge-intensive approach to fertilizer management can substitute for higher levels of inputs, saving farmers money and reducing environmental costs.

Agricultural intensification through the use of high-yielding crop varieties, chemical fertilizers and pesticides, irrigation, and mechanization—known as the "Green Revolution"—has been responsible for dramatic increases in grain production in developing countries over the past three decades. At the same time, intensification has had environmental consequences such as leaching of nitrate and pesticides, and emissions of environmentally important trace gases. We evaluated the economic and agronomic consequences, and the effects on N trace gas, of fertilizer management in irrigated spring wheat systems in the Yaqui Valley, Sonora, Mexico. This region is one of Mexico's major breadbaskets, so agricultural production and its environmental consequences are regionally important. In addition, as the "home" of the Green Revolution for wheat, the pattern of increasing fertilizer use in the Yaqui Valley provides a gauge of what is likely to occur in other high-productivity irrigated cereal systems of the developing world (*1*, *2*).

P. A. Matson and R. Naylor, Institute for International Studies, Stanford University, Stanford, CA 94305–6055, USA.
I. Ortiz-Monasterio, International Maize and Wheat Improvement Center, El Batan, Mexico.
*To whom correspondence should be addressed.

Globally, application of fertilizer nitrogen (N) has increased rapidly in the last several decades, from 32 Tg N (32 million metric tons) in 1970 to around 80 Tg in 1990 (1 Tg = 10^{12} g); it is expected to increase to 130 to 150 Tg $year^{-1}$ by 2050, with two-thirds of that application in developing countries (*3*). Among the consequences of this change are increased losses of nitrate from soils to freshwater and marine systems and of N-containing gases to the atmosphere (*4*). Fertilized agriculture is the single most important anthropogenic source of N_2O, accounting for over 70% of the anthropogenic sources of this accumulating greenhouse gas (*5*, *6*). Likewise, fertilization results in elevated emissions of NO, a chemically reactive gas that regulates tropospheric ozone production and is a precursor to acid precipitation (*7*). Research in industrialized countries has shown that management practices can be used to control losses of N (*6*–*9*). However, integrated assessments of management alternatives in terms of their ability to reduce N trace gas fluxes and yet be feasible agronomically and attractive economically are wholly lacking. We carried out such an evaluation in the Yaqui Valley (*10*).

Using daily to weekly sampling frequencies during the 1994/1995 and 1995/1996 wheat cycles, we evaluated changes in soil nutrients and gas fluxes before and after fertilizer additions in experimental plots at the International Maize and Wheat Improvement Center (CIMMYT) field station (*11*). Several experimental conditions were studied: the conventional farmers' practice for the valley, as determined by farm survey (*12*); three alternative practices that were based on agronomist recommendations and that added less fertilizer N or fertilizer later in the crop cycle, or both (*13*); and a nonfertilized control. In our treatment that simulated the farmers' practice, 187 kg N/ha of urea were applied to dry soils 1 month beore planting, followed by preplanting irrigation; an additional 63 kg N/ha of anhydrous ammonia were applied ~6 weeks after planting.

After the soil was wetted by preplanting irrigation, ammonium (NH_4) levels increased markedly to over 600 μg/g (weighted average of bed and furrow positions) and then diminished to near zero as the microbially mediated process of nitrification converted NH_4 to nitrate (NO_3) (*14*, *15*). By the 1994 planting date, 116 kg/ha of NO_3-N were left in the top 15 cm of soil, with very little remaining in the NH_4 form. A similar pattern of transformation and loss was evident in the 1995/1996 wheat season.

Changes in N trace gas fluxes mirrored changes in the soil pools of inorganic N. The farmers' practice resulted in very large emissions of N_2O and NO in both years (Fig. 1), with preplanting gas fluxes summing to 5.6 and 4.6 kg N/ha in the 1994/1995 and 1995/1996 wheat cycles, respectively, and crop cycle fluxes summing to 6.61 and 11.3 kg N/ha, respectively (*16*, *17*). In the 1994/1995 study, average fluxes at midday in the bed positions (where most of the fertilizer was located) ranged up to 650 ng cm^{-2} $hour^{-1}$ for N_2O-N and 300 ng cm^{-2} $hour^{-1}$ for NO-N in the period before planting (*15*). In 1995/1996, which had less rainfall during the preplanting period, average N_2O and NO fluxes in the beds ranged up to 100 and 550 ng cm^{-2} $hour^{-1}$, respec-